

# Field-dependent electrical properties of carbon nanotubes from first-principles: negative differential conductance, current oscillations and molecular sensing

Jaime Silva<sup>1</sup> , Bruce F Milne<sup>1,2</sup>  and Fernando Nogueira<sup>1</sup> 

<sup>1</sup> CFisUC, Department of Physics, University of Coimbra, Rua Larga, 3004-516 Coimbra, Portugal

<sup>2</sup> Coimbra Chemistry Centre, Department of Chemistry, University of Coimbra, Rua Larga, 3004-535 Coimbra, Portugal

E-mail: [jaime.d.silva@uc.pt](mailto:jaime.d.silva@uc.pt), [bfmilne@uc.pt](mailto:bfmilne@uc.pt) and [fnog@uc.pt](mailto:fnog@uc.pt)

Received 3 October 2019, revised 20 November 2019

Accepted for publication 5 December 2019

Published 31 December 2019



## Abstract

In certain materials, and for certain voltage ranges, electrical current flowing through the material decreases when the voltage across the sample is increased. This negative differential conductance (NDC) is important for oscillators, amplifiers, and fast switching devices. In this work, using real time quantum simulations, we show that this phenomenon occurs in isolated finite armchair single wall carbon nanotubes (SWCNT) without end contacts. For metallic SWCNT, like the armchair SWCNT, electron transfer to secondary valleys—the most common cause of NDC—is not expected to be observed, as there are two quantum channels at the Fermi energy available for conduction. The NDC is due to the finite nature of the SWCNT and the existence of excited states that are blocked, similarly to a Coulomb blockade system, thus preventing any further current flow. We also show that the SWCNT conductivity depends on its length and that the current flowing on the SWCNT behaves like a Bloch oscillation that is disrupted in the presence of a molecule, decreasing the conductivity, and thus providing a rationalisation for the behaviour of SWCNT organic gas sensors.

Keywords: carbon nanotubes, density functional theory, time-dependent density functional theory, gas sensor, conductivity

(Some figures may appear in colour only in the online journal)

## Introduction

Since their discovery [1, 2] in the 90's, single wall carbon nanotubes (SWCNT) have become ubiquitous in the development of new types of materials. Their 1D electronic structure [3] enables the development of a vast range of electronic devices at the nanoscale.

The study of the conductivity of an isolated finite SWCNT without conductive terminals at both ends is important for a vast range of applications, a significant example of which is the use of SWCNT as sensors for organic gases [4]. These sensors are fabricated by distributing SWCNTs on an interdigitated electrode and can be used to detect gas and organic

vapours at room temperature. The SWCNT networks adsorb gas molecules causing a change in their conductivity. Li *et al* [4] proposed a phenomenological model that explains the change of the conductivity when organic gas molecules are adsorbed on the SWCNT. This model has its basis in two separate mechanisms. The first of these deals with intratube modulation, where it is assumed that there is a modulation of the Fermi level of the SWCNT upon adsorption of a molecule, resulting in changes to the SWCNT conductivity. The second invokes an intertube modulation, where there is the formation of a SWCNT-molecule-SWCNT junction where conduction can occur due to a hopping/tunnelling mechanism between SWCNTs in the network. Using this phenomenological

model, Li *et al* [4] explained their experimental results stating that in the case of *o*-nitrotoluene and benzene the intertube mechanism plays a crucial role, albeit they state that their observations are preliminary.

Negative differential conductance (NDC), also known as negative differential resistance, is an effect often exploited in oscillators, amplifiers, and fast switching devices [5, 6]. NDC occurs for some range of voltages, in some materials, and is simply the decrease in electrical current through the material when the voltage across it is increased. NDC has been observed in systems at the nanoscale like SWCNT based field-effect transistors [7, 8], graphene based field-effect transistors [9], single-molecule break junctions [10], two-dimensional metal-diboride ZrB<sub>2</sub> monolayers [11], MoS<sub>2</sub>–WS<sub>2</sub> lateral heterojunctions [12], and in Bose–Einstein condensates in an 1D optical lattice [13]. In general for devices at atomic scale the NDC is a result of tunneling through localised states [14]. For metallic SWCNT, like the armchair SWCNT, NDC due to electron transfer is not expected to be observed [15], a consequence of having two quantum channels at the Fermi energy available for conduction [3]. Interestingly, NDC has been observed for freely suspended metallic SWCNT at low electric fields [16], with the origin of the effect attributed to self-heating, i.e. the presence of high-energy phonons.

In the past NDC has been thoroughly studied in semiconductors such as GaAs and n-Ge. In these crystalline systems NDC is a result of scattering of the electrons from one band to another one where their effective mass is greater [15, 17, 18].

Time dependent density functional theory (TDDFT) [19, 20] was recently applied to demonstrate the existence of NDC in liquid aluminum [21]. In this work, the authors developed a methodology that enables that calculation of the conductivity and the current density in the framework of TDDFT. Moreover, it enables the calculation of the electrical conductivity of large finite macromolecules such as the SWCNT. It should be noted that the *ab initio* calculation of the electrical conductivity is usually performed using density functional theory (DFT) and the Kubo–Greenwood formula [22, 23], which is only suitable for low-current regimes, being thus unable to predict non-linear effects in the electrical conductivity. Accessing the non-linear regime of the conductivity might provide an answer to important questions such as, if the observed NDC is a ubiquitous effect at higher current densities [21] and what is the precise nature of the NDC.

By using a metallic SWCNT as prototype system we will show that NDC prevails at high current densities and by calculating the number of excited electrons we will argue that NDC is a consequence of a Coulomb blockade (CB) regime. Finally, we will demonstrate that finite armchair SWCNT display NDC at high electric fields due to their finite size. We will also show that the flow of current on the SWCNT behaves like a Bloch oscillation that is disrupted by adsorbed molecules, thus diminishing the SWCNT conductivity. This could explain how SWCNT based gas sensors work, elucidating the role of the intrinsic mechanism of the phenomenological model of Li *et al* [4].

**Table 1.** Values of the work function and conductivity obtained using DFT/TDDFT for different SWCNT systems.

System	$W_f$ (eV)	Conductivity (S cm <sup>-1</sup> )
SWCNT@(3,3)	4.412	51.947
SWCNT@(3,3) + Benzene	4.378	49.632
SWCNT@(3,3) + <i>o</i> -Nitrotoluene	4.378	48.762

## Theoretical methods

In this work we use DFT [24] and its time-dependent formulation, TDDFT [19], to calculate [25] the current density.

The single-particle Kohn–Sham (KS) DFT/TDDFT hamiltonian is given by

$$\hat{H}[n](t) = \frac{1}{2} \left( -i\nabla + \frac{1}{c} \mathbf{A}_{\text{ext}}(t) \right)^2 + \hat{v}[n](t) \quad (1)$$

where  $\mathbf{A}_{\text{ext}}$  corresponds to an external vector potential,  $n$  is the electronic density, and  $\hat{v}$  is the KS effective potential that can be decomposed into separate external, Hartree and exchange-correlation potentials.

In our calculations the DFT/TDDFT equations were discretised over a uniform real-space grid with a spacing of 0.20 Å. The simulation box was constructed from atom-centred spheres of radius 3.5 Å. The time step used for the evolution of the KS states was  $2.419 \times 10^{-5}$  fs, and the local density approximation to exchange and correlation was used [26–28].

Finite SWCNT were generated<sup>3</sup> with  $K = 5, 10, 15$  and 20 translations of the unit cell along the tube longitudinal axis and the terminal carbons of the finite SWCNT were passivated with hydrogens. For the results presented in table 1, we used a SWCNT with  $K = 15$ . All structures were optimised at the DFT level using the exchange-correlation functional of Tao *et al* (TPSS) [29] and including Grimme’s D3 dispersion corrections as provided by the ORCA 3.0.1 package [30]. The multiply-polarized triple- $\zeta$  Def2-TZVP basis set of Ahlrichs and co-workers was employed in all TPSS calculations [31]. For the infinite SWCNT we used a parallelepipedic super cell with dimensions (18.897, 18.897, 2.328) atomic units. Reciprocal space was sampled with a  $1 \times 1 \times 128$   $k$ -points grid.

In all of our presented computations we use as convergence criteria the density. We assume a value of  $1.0 \times 10^{-8}$  for the relative convergence of the density. For the convergence criteria of the optimization of the SWCNT, we use  $5.0 \times 10^{-6}$  Hartree for difference between the cycles of the self-consistent field and a gradient of  $3.0 \times 10^{-4}$  Hartree/Bohr with root mean square of the gradient of  $1.0 \times 10^{-4}$  Hartree/Bohr.

To calculate the conductivity we use the procedure described by Andrade *et al* [21]. In their work they use TDDFT to calculate the current density  $\mathbf{J}(t)$  due to an applied time dependent field  $\mathbf{E}(t)$ . In this method, the system is perturbed

<sup>3</sup> TubeGen 3.4 (web-interface, <http://turin.nss.udel.edu/research/tubegenonline.html>), Frey and Doren, University of Delaware, Newark DE, 2011.

by a kick, an electric field of the form  $\mathbf{E}(t) = \mathbf{E}_0(t)\delta(t)$  with  $\mathbf{E}_0$  determining the intensity and the direction of the field. In this work, the following range of values for  $\mathbf{E}_0$  was employed: 0.01, 0.05, 0.1, 0.5, 1.0, 1.5, 2.0, 2.5, 2.75, 3.0 and then steps of 0.5 until 5.0 (atomic units). Conductivity is calculated from the current density obtained from the TDDFT simulations as

$$\sigma(\omega) = \frac{1}{E_0} \int_0^\infty e^{-i\omega t} J(t) dt. \quad (2)$$

DC conductivity is determined by an exponential fit to  $J(t)$  ( $t < 0.03$  fs).

The number of excited electrons can be calculated from the time-dependent occupation number of the KS wave functions [32, 33]

$$M_j(t) = 2 \sum_k^{\text{occ}} |\langle \varphi_j(\mathbf{r}, 0) | \varphi_k(\mathbf{r}, t) \rangle|^2 \quad (3)$$

where  $\varphi_j(\mathbf{r}, 0)$  refers to the ground state KS wave functions and  $\varphi_k(\mathbf{r}, t)$  to the occupied time dependent KS wave functions. Hence the number of excited electrons is calculated using

$$N_{\text{exc}}(t) = N_{\text{total}} - \sum_j^{\text{occ}} M_j(t) \quad (4)$$

where  $N_{\text{total}}$  is the total number of electrons of the SWCNT. Finally, the work function is defined as the difference between the Fermi level and the vacuum level.

## Results and discussion

We used the procedure described by Andrade *et al* [21], applying an electrical pulse (the ‘kick’) that induces a current density (see the Theoretical Methods section). The resulting stream lines are initially straight and parallel to the applied electric field [21], as can be seen in figure 1 (Top) for the SWCNT with  $K = 15$ , a kick intensity of  $5.142 \times 10^7$  V cm<sup>-1</sup>, and 0.001 20 fs of time propagation.

After 0.037 49 fs (figure 1 (Bottom)) the previously linear stream lines are seen to oscillate around the carbon atoms. Periodic oscillation of the electrons in this manner, under an applied electric field and in a periodic potential, is termed a Bloch oscillation [26, 34]. For crystalline solids, these oscillations are a consequence of the periodicity [35]. In this case of a finite SWCNT it can be observed in figure 1 (Bottom) that the Bloch oscillations [26, 34] are induced by the periodicity in the potential resulting from the organisation of SWCNT carbon atoms in a finite lattice. The existence of Bloch oscillations in SWCNT has previously been predicted using a tight binding model [36].

Moreover, we expect that these oscillations to still be observed for metallic armchair (n,n) SWCNT with different diameters because the carbon–carbon distance remains constant (it is independent of the SWCNT diameter).

It is interesting to note that in the presence of another molecule in close proximity to the surface of the SWCNT, the regular pattern in the stream lines is altered, perturbing the

Bloch oscillations. This can be seen in figure 2 for the simple molecules benzene (Top) and *o*-nitrotoluene (Bottom).

The adsorption of organic molecules on the surface of the SWCNT is important for gas sensing applications as demonstrated by Li *et al* [4]. The details of the intrinsic mechanism of the gas sensor proposed by Li *et al* [4] have only been described in a phenomenological manner. In order to further investigate the role of the potential mechanisms in the phenomenological model of Li *et al* [4], the conductivity and the work function were calculated for a (3,3) SWCNT with benzene or *o*-nitrotoluene adsorbed on its surface. These were the organic molecules studied in Li *et al* [4]. The details of the structural models and their optimisation are described in the Theoretical Methods section.

In table 1 we present the values of the work function and conductivity, calculated using DFT/TDDFT, for different systems: an isolated SWCNT, and the same SWCNT with either benzene or *o*-nitrotoluene adsorbed on its surface. It is possible to see in table 1 that the perturbation of the Bloch oscillations by the adsorption of an organic molecule on the surface of a SWCNT, as shown in figure 2, will induce a change in the intrinsic conductivity of the SWCNT. In addition, the presence of the organic molecules leads to a reduction in the magnitude of the work function which will in practice lead to similar values for the conductance of the different systems. Finally, the values reported in table 1 corresponds to an  $E_0$  of 0.01 (atomic units) which ensures that the system is in the Ohmic regime and the electrons responsible for the surface plasmon are excited.

Knowing the work function, one can calculate the conductance due to tunneling between two SWCNT, i.e. tunneling between two similar electrodes separated by a thin insulating film [37],

$$g_{ij} = \frac{A\sqrt{2W_f}}{d_{\text{min}}} e^{-2\pi d_{\text{min}}\sqrt{2W_f}}. \quad (5)$$

In equation (5),  $A$  is the sectional area of the SWCNT (approximated by the square of the SWCNT diameter),  $W_f$  is the work function and  $d_{\text{min}}$  is the minimal distance between a given pair ( $ij$ ) of SWCNT. All quantities are to be expressed in atomic units.

If we build a network where the nodes are the SWCNT and the edges are resistances with the value defined by equation (5) plus the intrinsic SWCNT resistance, we can calculate the conductivity of the whole system [38].

If the adsorbed molecule would induce a change in the work function, the conductivity between SWCNT would be altered. This would correspond to the intertube modulation proposed by Li *et al* [4]. If, on the other hand, the adsorbed molecule would lead to a change in the SWCNT conductivity, corresponding to the intratube modulation of Li *et al* [4].

In order to investigate further the role of the two potential mechanisms in the phenomenological model of Li *et al* [4] we developed a theoretical study based on network theory [38]. First a set of hard cylinders with an aspect ratio, the ratio between length and diameter, of 100 are randomly position on a 3D domain with periodic boundary conditions until a volume fraction, the ratio of the volume of the cylinders to the

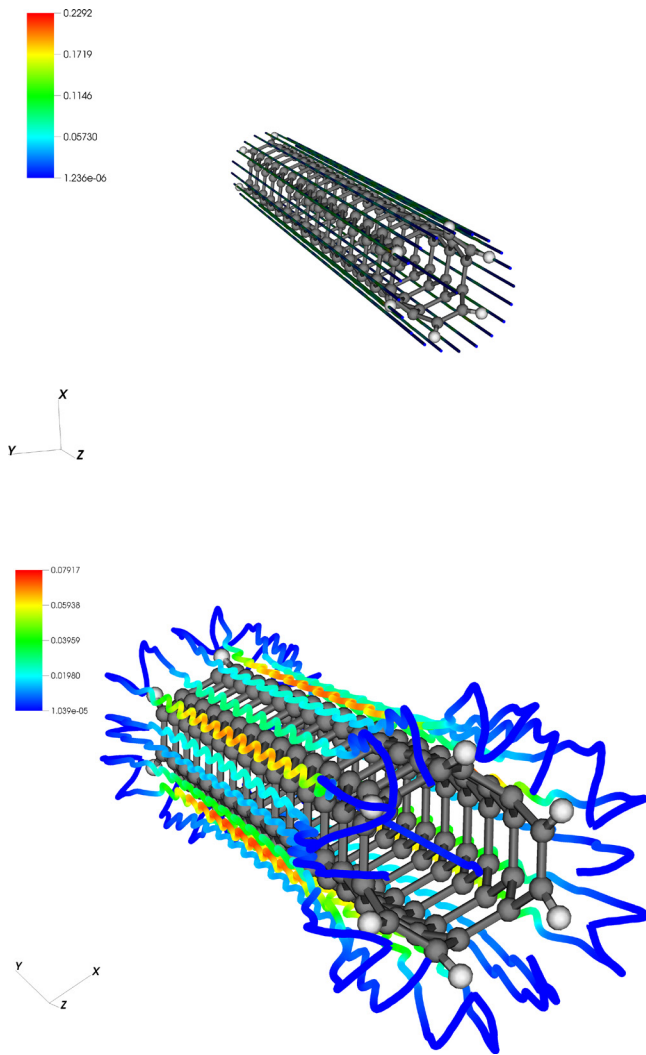


**Figure 1.** (Top) Stream lines for an initial kick  $E_0 = 5.142 \times 10^7$  V cm<sup>-1</sup> after 0.001 20 fs. (Bottom) The same stream lines at  $t = 0.037$  49 fs.

total volume of the domain, of 0.011 is achieved. Secondly, a resistance network is created using equation (5) plus the intrinsic resistance of the SWCNT and the conductance is extracted using the matrix representation for a resistor network and Kirchhoff's current laws [39]. Finally, the conductance is averaged over 500 samples ensuring that the standard deviation for the conductivity is less than 0.001 (S). To study the effect of the intertube modulation in the system conductivity we fixed the nanotube conductivity and varied the work function, calculated using DFT as presented in table 1. To study the intratube modulation we fixed the work function and use the values for SWCNT conductivity calculated using TDDFT and presented in table 1. The latter studies are presented in table 2, column two for the intertube study and column three for the intratube, as a change in the conductivity were  $\sigma_0$  represents the SWCNT network without adsorbed molecules and  $\Delta$  is difference between the SWCNT+Benzene or *o*-Nitrotoluene and  $\sigma_0$ .

The results presented in table 2 indicate that the magnitude of the change in the conductivity obtained using equation (5) with the work function held constant is significantly larger (3

and 31 times greater respectively) than when the tube conductivity remains fixed and we vary the work function.

This leads to the conclusion that the intratube modulation, i.e. the change in the conduction of individual SWCNT caused by adsorption of analyte molecules, proposed by Li *et al* [4] is the main mechanism of their gas sensor.

The method of Andrade *et al* [21] that we have used in this work, requires the application of a 'kick', an electrical field of the form  $\vec{E}(\vec{r}, t) = \vec{E}_0\delta(t)$ . The constant vector  $\vec{E}_0$  determines the intensity and direction of the field, while the delta function ensures that this field excites all modes with the same intensity. In this work, we considered just one direction for  $\vec{E}_0$ , which means that we treated the conductivity as a scalar, not as a tensor. The use of a kick allows for the clear separation between external (macroscopic and controlled) and induced fields, as the former only exist at  $t = 0$ . Obviously, for different external fields, we will get different responses.

Some quantities, however, are reasonably independent of this field. Figure 3 shows the number of conduction electrons, i.e. the ratio between the current density and the initial kick scaled with the number of electrons of the system, as proposed by Andrade *et al* [21]. This number remains almost constant as the kick intensity is increased.

Figure 3 also shows that the number of conduction electrons decreases with the increase of SWCNT length, attaining its minimum for the infinite SWCNT. As was shown in Silva *et al* [40], the different responses of finite and infinite SWCNT can be traced back to the presence of a surface plasmon in the finite tubes. The energy of this surface plasmon decreases with increasing length of the SWCNT and this can explain the lower conduction electron count of longer tubes. As this surface plasmon is not present in the infinite case, the number of conduction electrons can be expected to be minimal in this case, as can be seen in figure 3.

Contrary to the number of conduction electrons, conductance depends quite strongly on the kick intensity, as can be seen in figure 4. The effect of SWCNT length on conductance is also shown in figure 4. Conductance diminishes with the increase of the length of the SWCNT, as expected. In the work of [41], it was suggested that transport through the nanotube was dominated by a single localised region the size of the length of the nanotube, corresponding to single molecular orbitals carrying the current and extending over the length of the nanotube [42]. In figure 5, we plot the current density over sections of the nanotube parallel and transverse to its length. The plots are for a (3,3)@SWCNT with  $K = 15$ , length = 35.75 and radius = 3.04 Angstrom 0.037 49 fs after the application of an initial kick. The  $z = 0$  plane corresponds to the middle of the tube. Conduction is clearly filamentary and the effect of a higher kick intensity seems to be the increase of the width of the filaments. This is in tune with the behaviour of bulk systems described by Ridley [5] and Volkov [6]. Increase in conductance with kick intensity could then be associated to the increase in the width of these filaments. Moreover, this process has an energy barrier because the existing filaments must reorganize themselves to accommodate the increase in the width. It is possible to observe this process by comparing

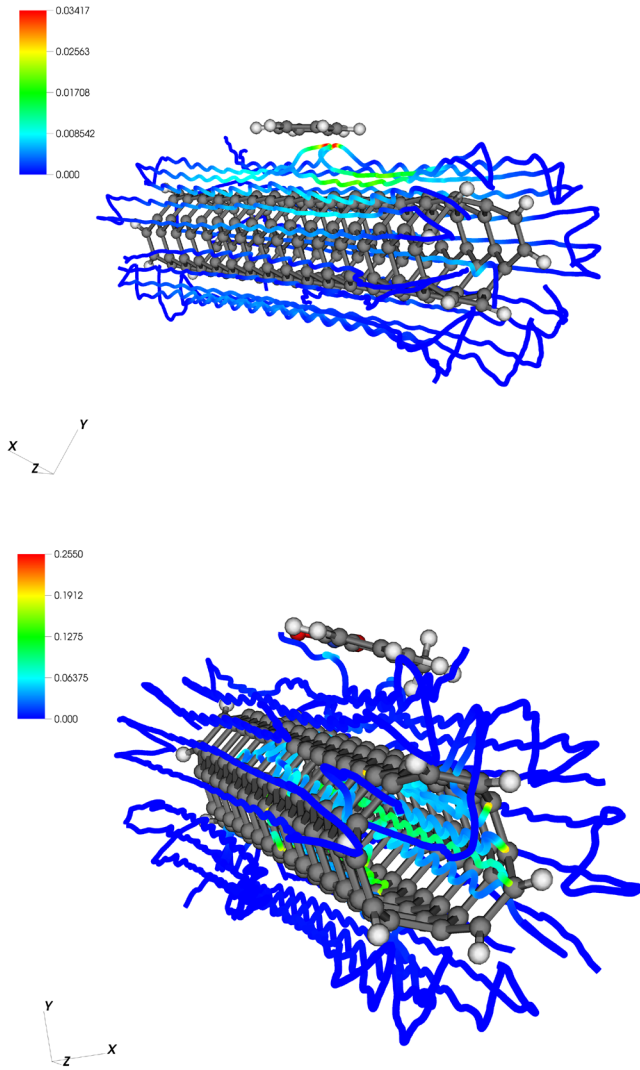


**Figure 2.** (Top) Stream lines for a system composed of a (3,3) SWCNT with an adsorbed benzene molecule 0.037 49 fs after the application of an initial kick,  $E_0 = 5.142 \times 10^7 \text{ V cm}^{-1}$ . (Bottom) Stream lines for a system composed of a (3,3) SWCNT with an adsorbed *o*-nitrotoluene molecule 0.037 49 fs after the application of an initial kick,  $E_0 = 5.142 \times 10^7 \text{ V cm}^{-1}$ .

**Table 2.** Values for the change in the network conductivity for the different values of the work function and fixed SWCNT conductivity (column two) and for the different SWCNT conductivities and fixed work function (column three).

System	$\frac{\Delta\sigma_{WF}}{\sigma_0}$	$\frac{\Delta\sigma_{TDDFT}}{\sigma_0}$
SWCNT@(3,3) + Benzene	-0.014	-0.042
SWCNT@(3,3) + <i>o</i> -Nitrotoluene	-0.002	-0.062

figures 5(b) and (d) for the different kick intensities, before and after the rapid increase.

In figure 6 we plot current density versus total electric field for SWCNT with different lengths. Data points were obtained going through different kick intensities, and getting current density and conductivity of the SWCNT for each kick intensity. From these two quantities, and assuming the microscopic form of Ohm’s law, we calculated the total electric field. This field results from both the kick and the induced field.

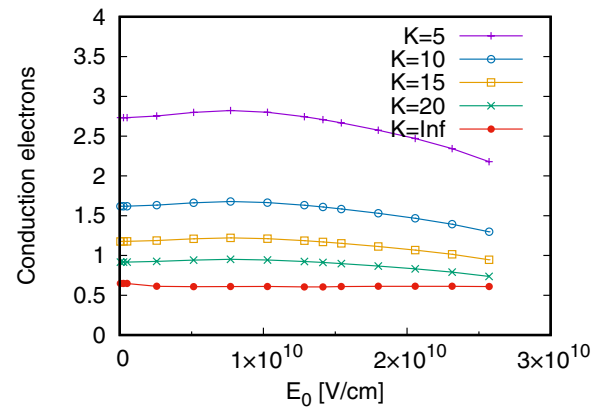


**Figure 3.** Number of conduction electrons versus kick intensity for SWCNT with different lengths.

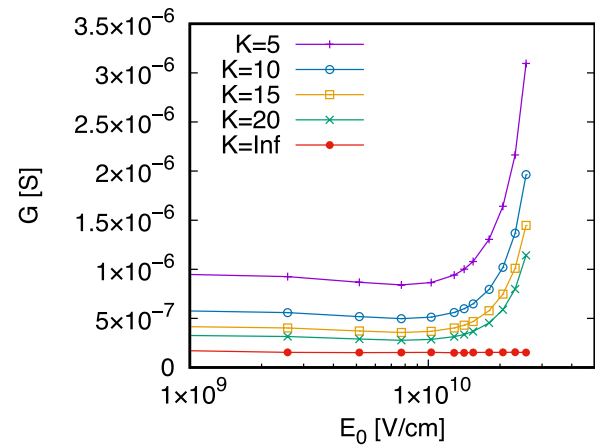


**Figure 4.** Conductance versus kick intensity for SWCNT with different lengths.

The figure shows that different values of  $E_0$  lead to identical values for the total electric field and to different values for the conductivity (as was already seen in figure 4). The SWCNT thus exhibit NDC at very high fields. These very high currents seem physically impossible, and it is also doubtful that nanotubes will be able to withstand them. We can, however, conjecture that the development of sub-attosecond lasers will permit the obtention of these high fields at the nanoscale. And the experimental results of Yao *et al* [43], that measured current densities in excess of  $10^9 \text{ A cm}^{-2}$ , prove that nanotubes can withstand very high currents. Even though the fields applied to the infinite nanotube were higher than those applied to the finite nanotubes, our results indicate that NDC is exclusive of the finite tubes. Furthermore, our results for the infinite SWCNT, the linear relation between current density and electric field, follows a similar theoretical work [44] that uses Landauer formalism to calculate the  $I$ - $V$  curves of (n,n) SWCNT.

Figure 6 also indicates that the onset of NDC is length dependent, diminishing as the length of the SWCNT increases. Our results also show that NDC in finite SWCNT is of the S (or current-controlled) type [5].

Studies on transport through a nanotube depend on the existence of source and drain electrodes connected to the ends of the

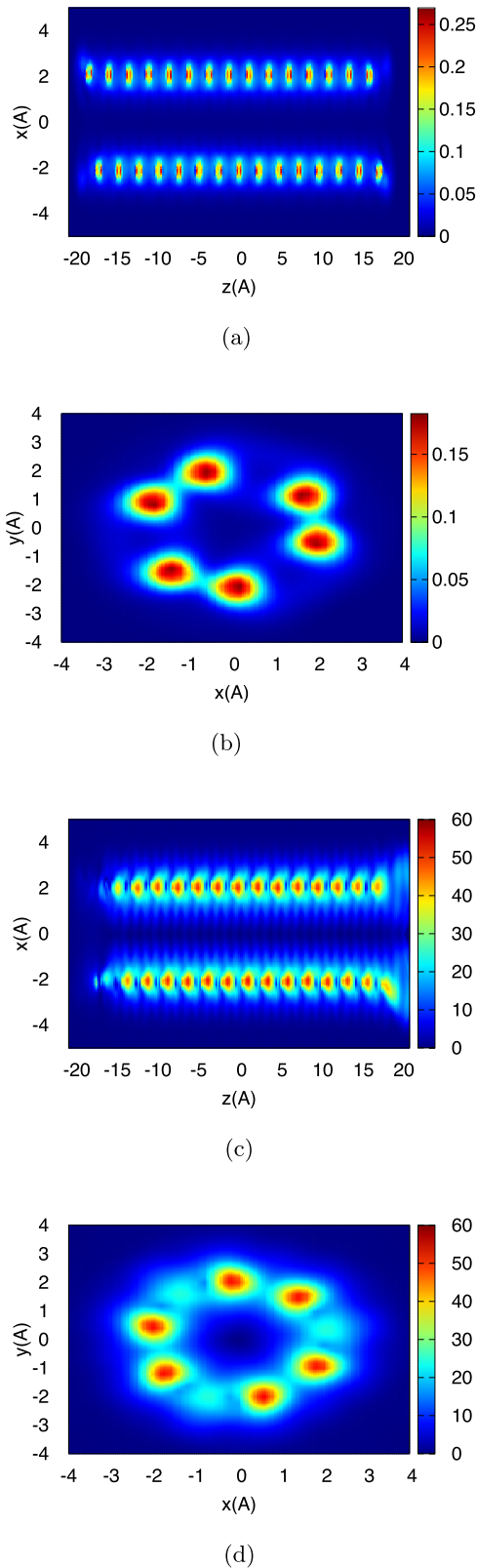


**Figure 5.** Current density profile in different planes and for different kick intensities for the SWCNT. (a)  $E_0 = 0.01$ ,  $y = 0$  plane. (b)  $E_0 = 0.01$ ,  $z = 0$  plane. (c)  $E_0 = 3.5$ ,  $y = 0$  plane. (d)  $E_0 = 3.5$ ,  $z = 0$  plane.

SWCNT. In our work, there are no such electrodes. However, vacuum can be seen as a virtual electrode. Our system can thus be considered a molecule weakly coupled to a drain electrode.

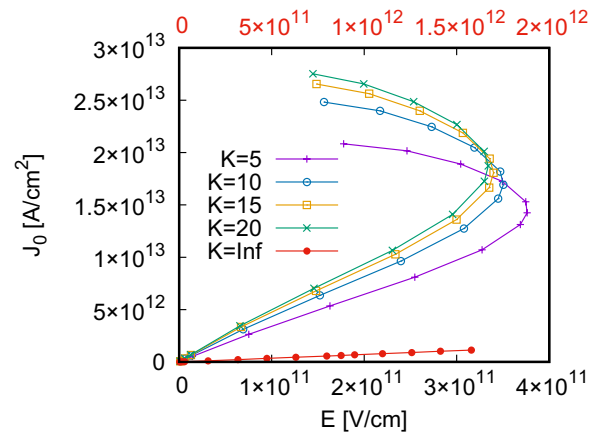


**Figure 6.** Current density versus electric field for SWCNT with different lengths. Data points correspond to the following sequence of kick intensities:  $E_0 = 0.01, 0.05, 0.1, 0.5, 1.0, 1.5, 2.0, 2.5, 2.75, 3.0, 3.5, 4.0, 4.5, 5.0$  (atomic units). The lines connecting the dots are just guiding the eye, as they simply follow the sequence of values for  $E_0$ . The red horizontal scale corresponds to the infinite SWCNT.

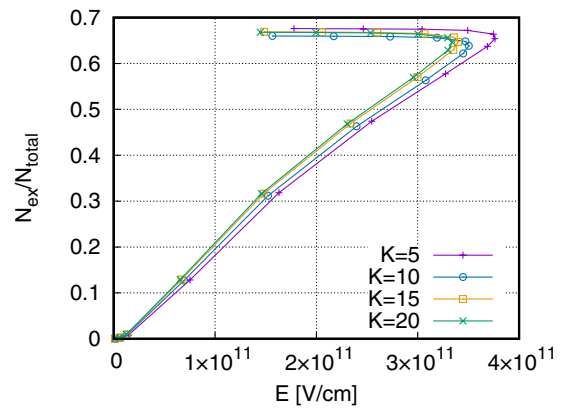


**Figure 7.** Fraction of excited electrons versus total electric field for SWCNT with different lengths.

A model for NDC due to a CB regime in a molecular junction was proposed by Muralidharan and Datta [45] and further explored by Xu and Dubi [46]. In their work, a molecular junction is generically modelled by its HOMO and LUMO levels. At zero bias, and with the molecule weakly coupled to the electrodes, the HOMO level is initially occupied and the LUMO unoccupied. On application of an electric field the LUMO levels become occupied due to excitation of electrons across the HOMO-LUMO gap. As these two levels cannot be occupied simultaneously, because of the Coulomb charging energy, occupation of the LUMO will decrease the HOMO population.

Electrons are emptied from the LUMO or from the HOMO levels to the vacuum, our virtual drain electrode. However, due to the increase of the electric field the HOMO/LUMO gap also increases, blocking the excitations of the HOMO electrons. This leads to a situation where the current is only due to the HOMO electrons and hence the current is observed to decrease with the increase of the electric field leading to the NDC behaviour.

In order to confirm that excitations of the HOMO electrons are indeed blocked, we plotted the fraction of excited electrons

versus total electric field (figure 7). In the region where NDC is observed, the fraction of excited electrons remains constant. This confirms the conclusion that the excited states are blocked, preventing the excitation of electrons and leading to a decrease of the current density.

## Conclusion

In this work, using real time quantum simulations, we show that finite armchair SWCNT display NDC. The effect originates in the finite nature of the SWCNT and in the inhibition of electronic excitations which prevents any further current flow. Moreover, we find that SWCNT conductivity depends on its length. It is also shown that the current flowing on the SWCNT behaves like a Bloch oscillation and that in the presence of a molecule adsorbed on the SWCNT the regular oscillatory pattern of this flow is disrupted, decreasing the conductivity. This reduction of the conductivity provides a theoretical rationale for the behaviour of SWCNT organic gas sensors, fabricated by distributing SWCNTs on an interdigitated electrode, which was previously explained phenomenologically. We show that intratube modulation, i.e. the change in the conduction of individual SWCNT caused by adsorption of analyte molecules, proposed by Li *et al* [4], is the main mechanism of their gas sensor.

## Acknowledgments

Computer time for this work was provided by the Laboratory for Advanced Computing (LCA) of the University of Coimbra. The authors thank the Fundação para a Ciência e a Tecnologia for financial support under project CENTRO-01-0145-FEDER-000014, 2017–2020 (JS and BFM), project POCI-01-0145-FEDER-032229 (BFM) and contract CEECIND/00579/2017 (JS).

We also acknowledge project PTDC/FIS-MAC/32229/2017, funded by the Portuguese National Budget through Fundação para a Ciência e Tecnologia/MCTES and also funded by the European Regional Development Fund (ERDF) through the Competitiveness and Internationalisation Operational Programa (PT-COMPETE 2020).

The Coimbra Chemistry Centre is supported by Fundação para a Ciência e a Tecnologia, through the Project PEst-OE/QUI/UI0313/2014 and POCI-01-0145-FEDER-007630.

## ORCID iDs

Jaime Silva  <https://orcid.org/0000-0002-1520-0799>

Bruce F Milne  <https://orcid.org/0000-0002-5522-4808>

Fernando Nogueira  <https://orcid.org/0000-0003-3125-3660>

## References

- [1] Iijima S 1991 *Nature* **354** 56
- [2] Odom T W, Huang J-L, Kim P and Lieber C M 1998 *Nature* **391** 62
- [3] Charlier J-C, Blase X and Roche S 2007 *Rev. Mod. Phys.* **79** 677
- [4] Li J, Lu Y, Ye Q, Cinke M, Han J and Meyyappan M 2003 *Nano Lett.* **3** 929
- [5] Ridley B K 1963 *Proc. Phys. Soc.* **82** 954
- [6] Volkov A F and Kogan S M 1969 *Phys.—Usp.* **11** 881
- [7] Li J and Zhang Q 2005 *Carbon* **43** 667
- [8] Rinkiö M, Johansson A, Kotimäki V and Törmä P 2010 *ACS Nano* **4** 3356
- [9] Wu Y, Farmer D B, Zhu W, Han S-J, Dimitrakopoulos C D, Bol A A, Avouris P and Lin Y-M 2012 *ACS Nano* **6** 2610
- [10] Perrin M L *et al* 2014 *Nat. Nanotechnol.* **9** 830
- [11] An Y, Jiao J, Hou Y, Wang H, Wu R, Liu C, Chen X, Wang T and Wang K 2019 *J. Phys.: Condens. Matter* **31** 065301
- [12] An Y, Zhang M, Wu D, Fu Z and Wang K 2016 *J. Mater. Chem. C* **4** 10962
- [13] Labouvie R, Santra B, Heun S, Wimberger S and Ott H 2015 *Phys. Rev. Lett.* **115** 050601
- [14] Lyo I-W and Avouris P 1989 *Science* **245** 1369
- [15] Conwell E M 2008 *Nano Lett.* **8** 1253
- [16] Pop E, Mann D, Cao J, Wang Q, Goodson K and Dai H 2005 *Phys. Rev. Lett.* **95** 155505
- [17] Conwell E M 1967 *High Field Transport in Semiconductors* (New York: Academic)
- [18] McGroddy J, Nathan M and Smith J 1969 *IBM J. Res. Dev.* **13** 543
- [19] Runge E and Gross E K U 1984 *Phys. Rev. Lett.* **52** 997
- [20] Marques M, Maitra N, Nogueira F, Gross E K U and Rubio A 2012 *Fundamentals of Time-Dependent Density Functional Theory (Lecture Notes in Physics)* (Berlin: Springer)
- [21] Andrade X, Hamel S and Correa A A 2018 *Eur. Phys. J. B* **91** 229
- [22] Kubo R 1957 *J. Phys. Soc. Japan* **12** 570
- [23] Greenwood D A 1958 *Proc. Phys. Soc.* **71** 585
- [24] Hohenberg P and Kohn W 1964 *Phys. Rev.* **136** B864
- [25] Andrade X *et al* 2015 *Phys. Chem. Chem. Phys.* **17** 31371
- [26] Bloch F 1929 *Z. Phys.* **52** 555
- [27] Dirac P A M 1930 *Math. Proc. Camb. Phil. Soc.* **26** 376
- [28] Perdew J P and Zunger A 1981 *Phys. Rev. B* **23** 5048
- [29] Tao J, Perdew J P, Staroverov V N and Scuseria G E 2003 *Phys. Rev. Lett.* **91** 146401
- [30] Neese F 2012 *Wires Comput. Mol. Sci.* **2** 73
- [31] Weigend F and Ahlrichs R 2005 *Phys. Chem. Chem. Phys.* **7** 3297
- [32] Miyauchi S and Watanabe K 2017 *J. Phys. Soc. Japan* **86** 035003
- [33] Otobe T, Yamagiwa M, Iwata J-I, Yabana K, Nakatsukasa T and Bertsch G F 2008 *Phys. Rev. B* **77** 165104
- [34] Zener C 1934 *Proc. R. Soc. A* **145** 523
- [35] Geiger Z A *et al* 2018 *Phys. Rev. Lett.* **120** 213201
- [36] Jódar E, Pérez-Garrido A and Rojas F 2009 *J. Phys.: Condens. Matter* **21** 212202
- [37] Simmons J G 1963 *J. Appl. Phys.* **34** 1793
- [38] Silva J, Simoes R, Lanceros-Mendez S and Vaia R 2011 *Europhys. Lett.* **93** 37005
- [39] Silva J, Ribeiro S, Lanceros-Mendez S and Simões R 2011 *Compos. Sci. Technol.* **71** 643
- [40] Silva J, Oliveira M J T, Lanceros-Mendez S and Nogueira F 2016 *J. Phys. Chem. C* **120** 18268
- [41] Bockrath M 1997 *Science* **275** 1922
- [42] Tans S J, Devoret M H, Dai H, Thess A, Smalley R E, Geerligs L J and Dekker C 1997 *Nature* **386** 474
- [43] Yao Z, Kane C L and Dekker C 2000 *Phys. Rev. Lett.* **84** 2941
- [44] An Y, Sun Y, Jiao J, Zhang M, Wang K, Chen X, Wu D, Wang T, Fu Z and Jiao Z 2017 *Org. Electron.* **50** 43
- [45] Muralidharan B and Datta S 2007 *Phys. Rev. B* **76** 035432
- [46] Xu B and Dubi Y 2015 *J. Phys.: Condens. Matter* **27** 263202